Original Article

MOLECULAR METABOLISM

Thioalbamide inhibits F_0F_1-ATPase in breast cancer cells and reduces tumor proliferation and invasiveness in breast cancer *in vivo* models

L. Frattaruolo [1,,3], R. Malivindi [1,3], M. Brindisi [1], V. Rago [1], R. Curcio [1], G. Lauria [1], M. Fiorillo [1], V. Dolce [1], A.W. Truman [2], A.R. Cappello [1,*]**

ABSTRACT

Objective: Thioalbamide is a ribosomally synthesized and post-translationally modified peptide (RiPP) belonging to the family of thioamitides, a rare class of microbial specialized metabolites with unusual post-translational modifications and promising biological activities. Recent studies have demonstrated the ability of thioalbamide to exert highly selective cytotoxic effects on tumor cells by affecting their energy metabolism, thus causing abnormal ROS production and triggering apoptosis. This study is aimed to investigate the molecular mechanisms underlying the antitumor activity of thioalbamide in order to identify its exact molecular target.

Methods: Wild type MCF-7 and MDA-MB-231 breast cancer cell lines as well as cancer cells deprived of mitochondrial DNA (ρ^0 cells) were employed in order to assess thioalbamide effects on tumor bioenergetics. In this regard, metabolic profile was evaluated by a Seahorse XFe96 analyzer, and the activity of the enzyme complexes involved in oxidative phosphorylation was quantified by spectrophotometric assays. Thioalbamide effects on tumor invasiveness were assessed by gelatin zymography experiments and invasion assays. *In vivo* experiments were carried out on breast cancer xenograft and "experimental metastasis" mouse models.

Results: Experiments carried out on ρ^0 breast cancer cells, together with Seahorse analysis and the application of spectrophotometric enzymatic assays, highlighted the ability of thioalbamide to affect the mitochondrial respiration process, and allowed to propose the F_0F_1-ATPase complex as its main molecular target in breast cancer cells. Additionally, thioalbamide-mediated OXPHOS inhibition was shown, for the first time, to reduce tumor invasiveness by inhibiting metalloproteinase-9 secretion. Furthermore, this study has confirmed the antitumor potential of thioalbamide in two different *in vivo* models. In particular, experiments on MCF-7 and MDA-MB-231 xenograft mouse models have confirmed *in vivo* its high antiproliferative and pro-apoptotic activity, while experiments on MDA-MB-231 ″experimental metastasis" mouse models have highlighted its ability to inhibit breast cancer cell invasiveness.

Conclusions: Overall, our results shed more light on the molecular mechanisms underlying the pharmacological potential of thioamidated peptides, thus reducing the gap that separates this rare class of microbial metabolites from clinical studies, which could validate them as effective tools for cancer treatment.

Keywords Oxidative phosphorylation; Metabolism; Breast cancer; Thioamitides; RiPPs

1. INTRODUCTION

Thioalbamide is a ribosomally synthesized and post-translationally modified peptide (RiPP) belonging to the thioamitide family [1]. This rare class of microbial specialized metabolite includes peptides produced by different microorganisms, with different amino acid sequences but in which several specific chemical characteristics are preserved such as a macrocycle closed by an aminovinyl cysteine (AviCys) residue, a dimethylated histidine residue that gives the molecules a net positive charge, and the presence of several thioamide groups in place of backbone amide groups in the linear portion of the molecule [2]. The progenitor of this family of microbial peptides is

[1]Department of Pharmacy, Health and Nutritional Sciences, University of Calabria, Via P. Bucci, 87036 Rende (CS), Italy [2]Department of Molecular Microbiology, John Innes Centre, Colney Lane, Norwich, NR4 7UH, United Kingdom

[3] These authors contributed equally to this work.

*Corresponding author. E-mail: annarita.cappello@unical.it (A.R. Cappello).

**Corresponding author. E-mail: luca.frattaruolo@unical.it (L. Frattaruolo).

Abbreviations: RiPP, ribosomally synthesized and post-translationally modified peptide; AviCys, aminovinyl cysteine; ROS, reactive oxygen species; mtDNA, mitochondrial DNA; nDNA, nuclear DNA; SRB, sulforhodamine B; OXPHOS, oxidative phosphorylation; TTFA, tenoyl trifluoroacetone; OCR, oxygen consumption rate; FCCP, carbonyl cyanide-p-trifluoromethoxyphenylhydrazone; PMA, phorbol 12-myristate 13-acetate; IR, infrared; ABC/HP, avidin-biotin complex/horseradish peroxidase; ABC/AP, avidin-biotin complex/alkaline phosphatase; DAB, diaminobenzidine; MMPs, matrix metalloproteinases; ρ^0 cells, cells depleted of mtDNA

Received July 27, 2022 • Revision received December 7, 2022 • Accepted January 11, 2023 • Available online 16 January 2023

https://doi.org/10.1016/j.molmet.2023.101674

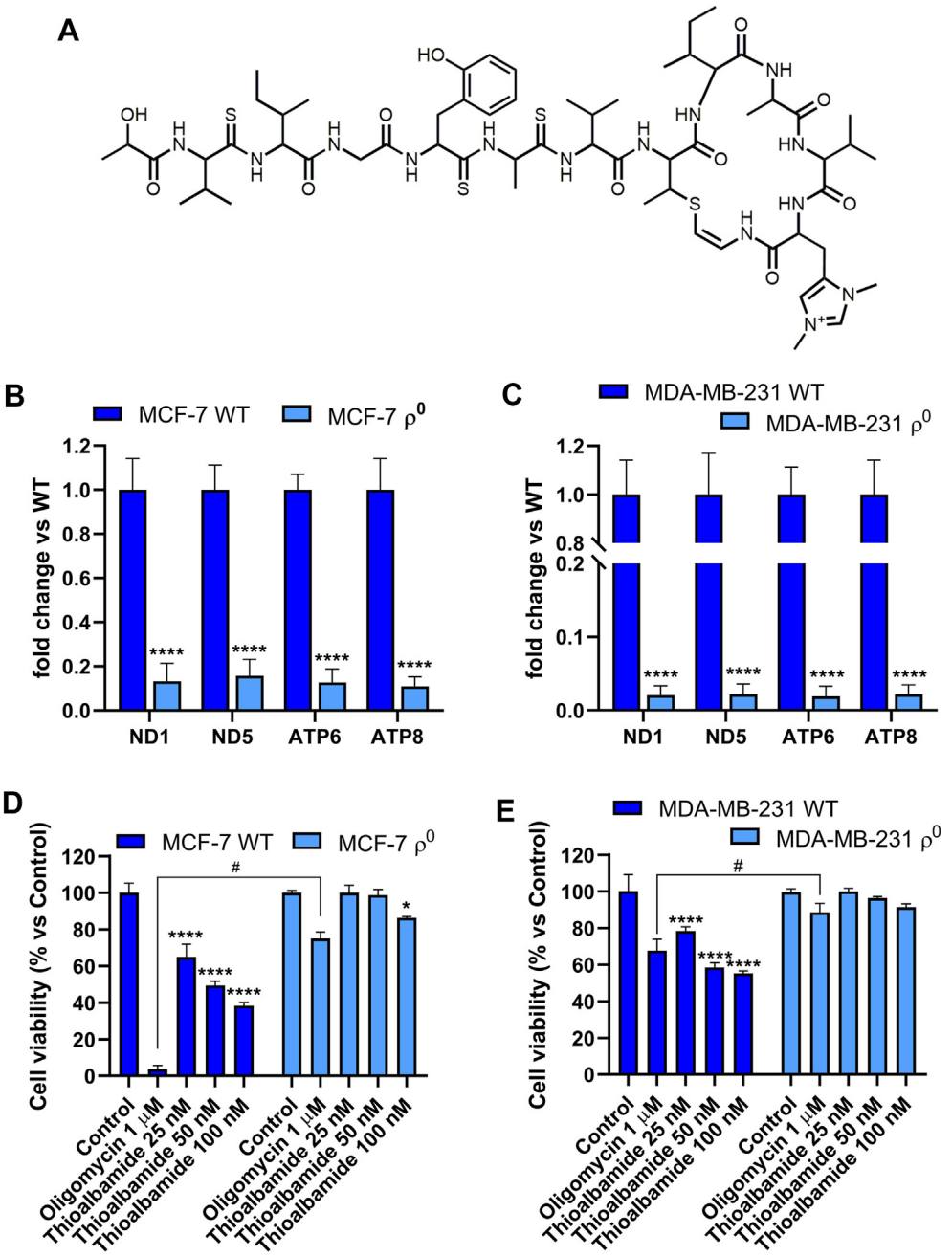

Figure 1: Thioalbamide activity requires functional oxidative phosphorylation. (A) Chemical structure of thioalbamide. MCF-7 (B) and MDA-MB-231 (C) cells were deprived of mtDNA (ρ^0) by treatment with ethidium bromide; mtDNA deprivation was verified by quantifying the mitochondrial genes ND1, ND5, ATP6 and ATP8 by qPCR. The effects of thioalbamide on WT and ρ^0 cell viability were assessed in MCF-7 (D) and MDA-MB-231 cells (E) by the SRB assay, after 72 h of treatment with increasing concentrations of the compound (25–100 nM). 1 μM oligomycin was used as positive control. Values represent mean ± SD of three independent experiments. *P value < 0.05, ****P value < 0.0001; #P value (oligomycin treatments) < 0.0001.

thioviridamide, isolated from the fermentation broth of *Streptomyces olivoviridis* NA05001 during a screening for antitumor antibiotics using 3Y1 rat fibroblasts transformed with adenovirus oncogenes [3,4]. Following the initial discovery of thioviridamide and its high, although poorly understood, cytotoxic potential, several new members of the thioamitide family have been isolated in recent years, such as thioalbamide from *Amycolatopsis alba* DSM 44262, thiostreptamide S4 from *Streptomyces sp.* NRRL S4, and thioholgamide A from *Streptomyces sp.* MUSC 136T [5,6]. The identification of this class of microbial specialized metabolite prompted biotechnological and pharmaceutical research to study different aspects of the thioamitides. Numerous works in recent years provided important information on the biosynthetic origin of these molecules, and on the enzymatic mechanisms underlying the extensive post-translational changes characterizing thioamitides [7–12]. Other studies have simultaneously investigated the biological potential of these peptides, highlighting the interesting cytotoxic activity that has grabbed the attention of cancer research [13–15].

Our study focused on thioalbamide (Figure 1A), which is characterized by a high anti-proliferative/cytotoxic activity, elicited at nanomolar concentrations, with a high selectivity towards tumor cells [5]. Recently, we demonstrated its ability to affect the energy metabolism of cancer cells, thus causing an increase in reactive oxygen species (ROS) production and triggering apoptotic cell death [13]. The interesting activity of thioalbamide at the metabolic level, although poorly characterized to date, is also responsible for its ability to target cancer stem-like cells, a tumor subpopulation characterized by high metabolic flexibility and often responsible for metastasis, as well as tumor recurrence and chemotherapy resistance [16]. In this paper, we investigate the molecular mechanisms underlying the antitumor activity of thioalbamide. In addition, we confirm *in vivo* the high antitumor potential of this microbial peptide, previously demonstrated *in vitro*, as well as to investigate, for the first time, its effects on the processes that mediate tumor invasiveness.

2. METHODS

2.1. Cell cultures

MCF-7 and MDA-MB-231 cell lines were purchased from the American Type Culture Collection (ATCC, Manassas, VA), and cultured in DMEM/F12 (Sigma Aldrich, St. Louis, MO) supplemented with 10% Fetal Bovine Serum (FBS, Sigma Aldrich), 2 mM L-glutamine (Sigma Aldrich) and 1% penicillin/streptomycin (Sigma Aldrich). ρ^0 cells were generated by treating MCF-7 and MDA-MB-231 cells with a low dose (25 ng/mL) of ethidium bromide (EtBr, Sigma Aldrich) for 30 days. ρ^0 cells were cultured in DMEM High Glucose (Sigma Aldrich), supplemented with 10% FBS (Sigma Aldrich), 2 mM L-glutamine, 1% penicillin/streptomycin, 100 μg/mL pyruvate (Sigma Aldrich) and 50 μg/mL uridine (Sigma Aldrich). Treatments were performed in the above-mentioned media containing a lower amount of serum (2%) or without serum (for gelatin zymography and invasion assays). All cell lines were cultured at 37 °C in 5% CO_2 in a humidified atmosphere. Thioalbamide was produced by fermentation of *A. alba* DSM 44262 and purified as previously described [5].

2.2. Mitochondrial DNA depletion assessment

Mitochondrial DNA (mtDNA) depletion in ρ^0 cells was assessed by quantitative real-time PCR, using a Quant Studio7 Flex Real-Time PCR System (Applied Biosystems) and SYBR Green Universal PCR Master Mix (Roche, Monza, Italy) according to manufacturer's recommendations. Total DNA from parental (WT) and ρ^0 MCF-7 and MDA-MB-231 cells was extracted as following. Cells were resuspended in SET buffer (75 mM NaCl, 25 mM EDTA pH 8, 20 mM Tris-HCl pH 7.5) and incubated with 500 μg/mL proteinase K and 1% SDS at 55 °C for 2 h. NaCl (1 M) was added to each sample, chloroform was added and samples were mixed for 30 min. The top layer from each sample was collected and mixed with 0.6 volumes of ice-cold isopropanol. Precipitated DNA was washed with 70% ethanol and then solubilized in DNAse-free water. RNA was eliminated by incubating samples with 100 μg/mL RNAse at 37 °C for 1 h. The mitochondrial genes ND1, ND5, ATP6 and ATP8 were used as targets for mtDNA quantification, and the nuclear gene coding for 18S rRNA was used to normalize mtDNA vs. nuclear DNA (nDNA). The primers used for amplifications are listed in Table 1.

Table1 – qPCR primers sequences.

Primer		Sequence
ND1	**Fw**	CCCTACTTCTAACCTCCCTGTTCTTAT
	Rev	CATAGGAGGTGTATGAGTTGGTCGTA
ND5	**Fw**	ATTTTATTTCTCCAACATACTCGGATT
	Rev	GGGCAGGTTTTGGCTCGTA
ATP6	**Fw**	GAAAATCTGTTCGCTTCATTCATTGCC
	Rev	ATCAGGTTCGTCCTTTAGTGTTGTG
ATP8	**Fw**	TACTACCGTATGGCCCACCA
	Rev	GCGAACAGATTTTCGTTCATTTTGGT
18S	**Fw**	AGTCGGAGGTTCGAAGACGAT
	Rev	GCGGGTCATGGGAATAACG

2.3. Cell viability assay

Sensitivity of WT and ρ^0 MCF-7 and MDA-MB-231 cells to thioalbamide or oligomycin was assessed by sulforhodamine B (SRB) assay. Briefly, 2×10^4 cells/well were seeded in 48-well plates and cultured overnight to allow cell attachment. Then, cells were treated with DMSO (control) or different concentrations of thioalbamide or oligomycin for 72 h. At the end of the treatment, cells were fixed with chilled 10% trichloroacetic acid for 15 min at 4 °C, washed with PBS and allowed to dry. Then, cells were stained with 0.04% SRB for 30 min and washed repeatedly with 1% acetic acid. The protein-bound dye was dissolved in 10 mM Tris and absorbance at 565 nm was quantified by using a microplate spectrophotometer (Synergy H1 microplate reader, BioTek).

2.4. Oxidative phosphorylation (OXPHOS) complexes activity assay

The enzymatic activity of the different electron transport chain complexes and F_0F_1-ATPase was assessed by using the MitoTox™ Complete OXPHOS Activity Assay Kit (Abcam, Cambridge, UK), which commonly allows for *in vitro* screening of the OXPHOS inhibitory activity of various compounds by means of spectrophotometric or colorimetric assays on the OXPHOS complexes isolated from bovine heart mitochondria, provided by the manufacturer. Rotenone, tenoyl trifluoroacetone (TTFA), antimycin A, potassium cyanide (KCN) and oligomycin (all from Sigma Aldrich) were used as positive controls of enzymatic activity inhibition.

2.5. Seahorse XFe96 metabolic profile analysis

MitoStress test was performed as previously described [17], by using the Seahorse XFe96 analyzer (Seahorse Bioscience, Billerica, MA, USA) on MCF-7 and MDA-MB-231 cells to detect variations in oxygen consumption rate (OCR) after sequential injections of oligomycin, FCCP and Rotenone/antimycin A. In order to test the metabolic effects of acute thioalbamide treatment, a modified MitoStress test was also performed by injecting 1 μM thioalbamide as a first injection before oligomycin. Results were analyzed by using the Software Wave Desktop Version 2.6.1, and normalized by SRB assay.

2.6. Gelatin zymography

In order to detect matrix metalloproteinase 9 (MMP-9) secreted by cancer cells, gelatin zymography experiments were performed. Breast cancer cells were seeded in 24-well plates (1×10^5 cells/well) and cultured overnight to allow cell attachment. Then, cells were treated for 24 or 48 h with DMSO (control) or thioalbamide in serum-free medium, in the presence or absence of 80 nM phorbol 12-myristate 13-acetate (PMA). At the end of the treatment, culture medium was collected from each sample, mixed with 4 volumes of acetone and incubated at −20 °C for 2 h to allow proteins precipitation. Pelleted proteins were solubilized in non-reducing sample buffer (4% SDS, 20% glycerol, 0.01% bromophenol blue, 125 mM Tris-HCl, pH 6.8) and loaded into a 7.5% poly-acrylamide gel containing 1 mg/mL gelatin. The gel was washed twice, for 30 min, with washing buffer (2.5% Triton X-100, 5 mM $CaCl_2$, 1 μM $ZnCl_2$, 50 mM Tris-HCl, pH 7.5) and incubated

overnight with incubation buffer (1% Triton X-100, 5 mM $CaCl_2$, 1 μM $ZnCl_2$, 50 mM Tris-HCl, pH 7.5) at 37 °C. After incubation, the gel was stained with Coomassie Blue solution (0.5% Coomassie Blue, 10% acetic acid, 40% methanol) and washed with a solution containing 10% acetic acid and 40% methanol before photographic acquisition.

2.7. Invasion assay

Cells were seeded in 24-well plates (1×10^5 cells/well) and cultured overnight to allow cell attachment. Then, cells were treated for 24 h with DMSO or thioalbamide, in serum-free medium, in the presence or absence of 80 nM PMA. At the end of the treatment, cells were detached from each well by trypsinization, washed and re-seeded onto the upper part of Boyden chambers (8 μm pores), previously coated with 30 μL of Matrigel (Sigma Aldrich) diluted 1:3 in serum-free medium. The upper part of the Boyden chamber was filled with serum-free medium, whereas the lower part was filled with 10% FBS containing medium. After 16 h the cells that invaded the lower part of the Boyden chamber septum were fixed and stained with Coomassie blue solution and observed by using an Olympus BX41 microscope with CSV1.14 software, using a CAMXC-30 for image acquisition.

2.8. *In vivo* xenograft mouse models

MCF-7 and MDA-MB-231 cells (5×10^6 cells/mouse) were ectopically inoculated in the interscapular region of 5/6-week-old athymic nude female mice ($n = 5$), under anesthesia induced by intraperitoneal injection of 250 mg/kg Avertin. In order to promote the growth of the estrogen-dependent MCF-7 cell line, an extended-release pellet of 17β-estradiol (0.72 mg per pellet, 90-day release; Innovative Research of America) was previously implanted in the dorso-lateral region of each mouse. Tumor development was monitored using a caliper, and tumor volume was calculated using formula $V = L(W)^2/2$ (where L is length and W is width). When tumors reached a volume of approximately 0.2 cm^3, mice were randomized and divided into groups, based on treatment. Mice were treated 3 times/week, by intraperitoneal administration of thioalbamide (0.5 mg/kg) or 0.9% NaCl (control groups) and tumor size was constantly monitored during the experiment. As previously described [18], at the end of the treatment period, animals were euthanized and tumor masses were isolated from the surrounding tissues, weighed, fixed in formalin and embedded in paraffin for subsequent histological analysis.

2.9. Generation of IR fluorescent cells

MDA-MB-231 infrared (IR) fluorescent cells were generated by performing a stable transfection of cells with pNLS-iRFP720, a gift from Vladislav Verkhusha (Addgene plasmid #45461; http://n2t.net/addgene:45461; RRID: Addgene_45461). Transfection was carried out using X-tremeGENE HP DNA Transfection Reagent (Sigma Aldrich), and G-418 (Sigma Aldrich) was used for selection of stable clones, whose fluorescence was confirmed using the Pearl Trilogy Small Animal Imaging System.

2.10. *In vivo* experimental metastases mouse models

IR fluorescent MDA-MB-231 cells (1×10^6 cells/mouse) were injected using a 28-gauge needle into the bloodstream of athymic nude female mice ($n = 5$), through the lateral caudal vein, dilated by immersing the tail of the anesthetized mouse in heated water. Mice were treated 3 times/week for 5 weeks, by intraperitoneal administration of thioalbamide (0.5 mg/kg) or 0.9% NaCl (Control groups). At the end of the treatment period, animals were euthanized and lung tissue was removed, following perfusion with 4% paraformaldehyde, checked for IR fluorescence (by using the Pearl Trilogy Small Animal Imaging System), and embedded in paraffin for subsequent histological analysis.

2.11. TUNEL assay

In order to assess apoptotic rate in tumors from *in vivo* experiments, TUNEL assay (Promega) was performed, according to manufacturer's recommendations, on 5 μm paraffin-embedded sections mounted on slides precoated with poly-lysine. Propidium iodide (Sigma Aldrich) was used for cell counterstaining, and fluorescence was evaluated by using the Olympus BX41 microscope with CSV1.14 software, using a CAMXC-30 for image acquisition.

2.12. Immunohistochemical analysis

Immunohistochemical experiments were carried out on paraffin-embedded sections (5 μm), mounted on slides precoated with poly-lysine, then they were deparaffinized and rehydrated (7—8 serial sections). After heat-mediated antigen retrieval, immunodetection was performed by incubating the slides with specific primary antibodies: anti-Ki-67 (1:100), anti-TOM20 (1:100) and anti-CD44 (1:100), overnight at 4 °C. Then, a universal biotinylated IgG (1:600) was applied for 1 h at room temperature, followed by avidin-biotin complex/horseradish peroxidase (ABC/HP, Vector Laboratories), for MCF-7 samples, or avidin-biotin complex/alkaline phosphatase (ABC/AP, Vector Laboratories) for MDA-MB-231 samples. According to the enzyme used for antibody labelling, immunoreactivity was visualized by using diaminobenzidine chromogen (DAB, Vector Laboratories) or Red-substrate (Vector Laboratories), for MCF-7 or MDA-MB-231 samples respectively. Immunostained tumor sections, counterstained with hematoxylin, were then evaluated by light microscopy using the Olympus BX41 microscope with CSV1.14 software, using a CAMXC-30 for image acquisition. Absorption controls utilized primary antibodies preadsorbed with an excess of their specific purified blocking peptide, at 4 °C for 48 h (data not shown). Ki-67 immunostaining was evaluated by light microscopy using the Allred Score [19], while TOM20 and CD44 immunoreactivity was scored as negative (−), weakly positive (+), moderately positive (++) or strongly positive (+++) by three independent observers [20].

2.13. Statistical analysis

GraphPad Prism 8 was used to conduct statistical analysis of all data. Statistical significance was evaluated by analysis of variance (ANOVA). A P value ≤ 0.05 was considered statistically significant. Normality of each distribution was confirmed by the Shapiro—Wilk test, while equality of variance was verified by Levene's test. Tukey's post-hoc test was used to study differences between groups.

3. RESULTS

3.1. Thioalbamide activity requires functional oxidative phosphorylation

Mitochondria play a key role in sustaining cellular functions by ATP production. The synthesis of ATP through oxidative phosphorylation represents the task that makes this organelle the engine of aerobic eukaryotic cells. Since preliminary results highlighted the ability of thioalbamide to affect mitochondrial metabolism, as well as to increase mitochondrial ROS production, we decided to evaluate whether the target of thioalbamide was located at the oxidative phosphorylation level. To this end, we generated breast cancer ρ^0 cell lines, which are deprived of mtDNA. Human mtDNA contains 37 genes: two genes coding for ribosomal RNAs (12S and 16S rRNAs), 22 genes coding for transfer RNAs (tRNAs), and 13 genes coding for polypeptides (mRNAs)

that make up some of the subunits of four of the five complexes of the mitochondrial respiratory chain. Without a functional respiratory chain, ρ^0 cells undergo metabolic reprogramming, by shifting their metabolism towards glycolysis, even in the presence of oxygen, in order to guarantee the tumor cell the energy needs for survival and proliferation.

Deprivation of mtDNA was achieved by prolonged cell incubation with ethidium bromide (EtBr), a DNA intercalating agent able to inhibit mtDNA replication. The specificity of ethidium bromide towards mtDNA is conferred by the net positive charge of the molecule, which preferentially accumulates in the negatively charged mitochondrial compartment. The resulting cells keep their nuclear genome intact and maintain their mitochondria, albeit with altered functionality, and can grow, *in vitro,* only in a culture medium enriched with glucose as a glycolytic substrate, as well as with uridine and pyruvate, an intermediate for the biosynthesis of amino acids and used to re-oxidize the excess of cytoplasmic NADH through the activity of lactate dehydrogenase [21].

Total DNA was isolated from WT cells and cells treated with EtBr to confirm the ρ^0 status. The mitochondrial genes ND1 and ND5, coding for two subunits of Complex I (NADH: ubiquinone oxidoreductase), as well as the ATP6 and ATP8 genes, coding for two subunits of F_0AT-Pase, were amplified by qPCR, and the relative quantification of mtDNA with respect to nDNA was performed by normalizing the results on the nuclear gene coding for ribosomal RNA 18S. The results obtained by real-time qPCR showed that mtDNA content in MCF-7 ρ^0 and MDA-MB-231 ρ^0 cells was drastically reduced when compared to the respective WT cells (Figure 1 panels B and C).

Once ρ^0 cells depleted of mtDNA were obtained and verified, their sensitivity to the cytotoxic action of thioalbamide was evaluated. Hence, MCF-7 and MDA-MB-231 wild type and ρ^0 cells were treated with different concentrations of thioalbamide, then cell viability was evaluated after 72 h by the SRB assay and compared to control cells treated with DMSO alone. Oligomycin treatment was used as positive control, to confirm the actual reduced sensitivity of ρ^0 cells to OXPHOS inhibitors. As shown in Figure 1 (panels D and E), MCF-7 ρ^0 and MDA-MB-231 ρ^0 cells were found to be much less sensitive to the cytotoxic action of thioalbamide than their respective WT lines, showing a similar behavior to that observed following oligomycin treatment. Although ρ^0 cells are characterized by mtDNA depletion and unpaired OXPHOS, other differences with parental cells cannot be excluded. However, such additional differences are mainly consequences of the unpaired OXPHOS function. For these reasons, our experimental evidences highlight that the cytotoxic action of thioalbamide requires the presence and integrity of mtDNA, thus suggesting that the molecular target of thioalbamide could be one of the enzyme complexes mediating cellular respiration and oxidative phosphorylation.

3.2. Thioalbamide affects oxidative phosphorylation by targeting F_0F_1-ATPase

Energy production in the mitochondrial compartment occurs at the level of the F_0F_1-ATPase complex, which synthesizes ATP by exploiting the proton motive force, in turn generated by the activity of the electron transport chain complexes. Indeed, mitochondrial respiration involves the transfer of electrons from NADH and $FADH_2$ along the electron transport chain to oxygen, which is reduced to H_2O, simultaneously accumulating H^+ ions in the intermembrane space. Protons re-enter the mitochondrial matrix through the F_0F_1-ATPase complex, thus determining the rotation catalysis that leads to ATP production. Since previous experiments suggested that thioalbamide could target oxidative phosphorylation, we evaluated its ability to inhibit the single complexes of the electron transport chain and the F_0F_1-ATPase complex. For this purpose, we used an OXPHOS Activity Assay Kit which usually allows to perform, by spectrophotometric enzymatic assays, a rapid *in vitro* screening of the potential inhibitory activity of several compounds on the OXPHOS complexes, from provided bovine heart mitochondria, which are immunocaptured in a multiwell plates. The activity of the individual complexes was evaluated at increasing concentrations of thioalbamide and, in parallel, a different known inhibitor was used as a positive control for each enzyme complex. In particular, for complex I rotenone was used, which interrupts electron transfer from NADH to ubiquinone; for complex II tenoyl trifluoroacetone (TTFA) was used, which binds to the reduction site of the quinone present in the enzyme complex, thus preventing ubiquinone from binding; for complex III antimycin A was used, which blocks electron transfer between cytochrome b and cytochrome c1, during the ubiquinone cycle (cycle Q); for complex IV potassium cyanide (KCN) was used; whereas oligomycin was used for the F_0F_1-ATPase complex. Our experiments showed that thioalbamide exerted a weak inhibitory action on the activity of complexes I and III but just at the highest concentration tested (10 μM), while no inhibition was found for the activity of complexes II and IV (Figure 2A). In contrast, the inhibitory effect exerted by thioalbamide on the F_0F_1-ATPase complex was noteworthy, as the latter was inhibited by more than 50% at a concentration of 100 nM. These results support our hypothesis on the ability of thioalbamide to act on the enzymatic complexes involved in the oxidative phosphorylation process, and are consistent with the similar inhibitory activity shown in recent studies by other thioamitides, such as prethioviridamide [15] and thioholgamide A [14].

The ability of thioalbamide to target oxidative phosphorylation in tumor cells was corroborated by carrying out a MitoStress Test, using a Seahorse analyzer, on MCF-7 and MDA-MB-231 cells. This test monitors changes in cellular oxygen consumption rate (OCR) following sequential injections of oligomycin, carbonyl cyanide-*p*-trifluoromethoxyphenylhydrazone (FCCP) and rotenone/antimycin. The response of breast cancer cells to a normal MitoStress test was compared to that of cells subjected to a modified test, in which thioalbamide was used as a first injection before oligomycin. The results obtained (Figure 2B, C) highlighted, both in MCF-7 and MDA-MB-231 cells, the ability of thioalbamide to determine a strong reduction of cellular OCR. The consequence of such phenomenon is reflected in a significant reduction of oligomycin effect, when it is added as a second injection. It is important to underline that the OCR levels achieved after the injection of oligomycin are fully comparable, both in the absence and in the presence of thioalbamide pre-injection. This result suggests that thioalbamide effect on cellular OCR does not add to that of oligomycin, but conversely the effect of both molecules could be elicited on the same target. Furthermore, the results obtained highlighted a maximal respiration rate which is unchanged in the presence of acute thioalbamide treatment, thus underlining that the effect observed in breast cancer cells exposed to this microbial peptide could be attributable to a highly specific inhibition against the F_0F_1-ATPase complex.

3.3. Thioalbamide affects MMP-9 secretion and tumor invasiveness

Next, we extended our investigation to the effect of thioalbamide on the invasiveness of tumor cells, a different aspect from those studied to date for this peptide or its natural analogues. In particular, the ability of thioalbamide to modulate the secretion of matrix metalloproteinases (MMPs) was evaluated for the first time. MMPs are a family of zinc-dependent endoproteinases involved in the degradation of the extracellular matrix (ECM), which, when uncontrolled, turns out to be a

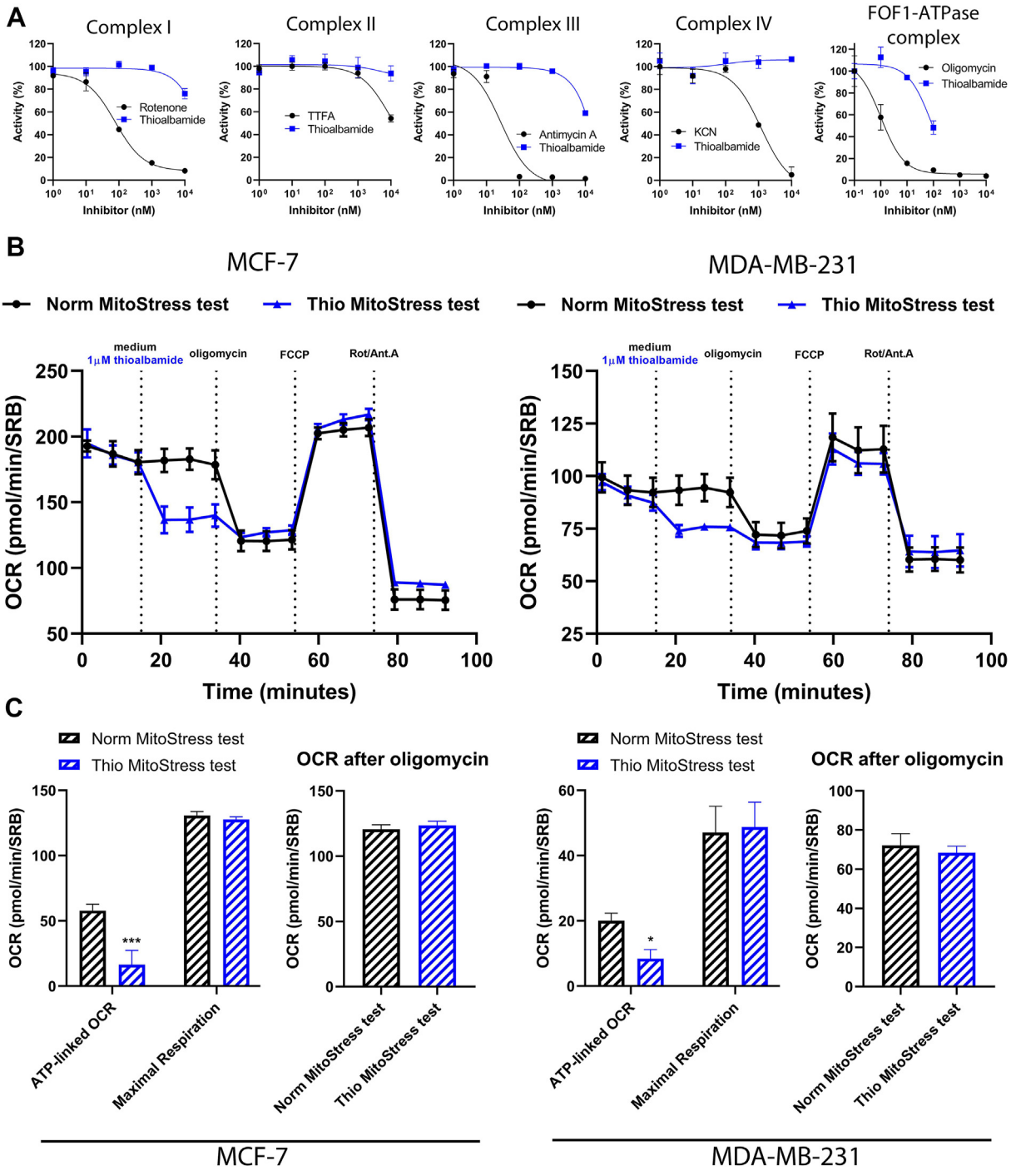

Figure 2: Thioalbamide inhibits oxidative phosphorylation. (A) The inhibitory activity of thioalbamide, as well as that of known mitochondrial inhibitors, was assessed spectrophotometrically on the different complexes of the respiratory chain and F_0F_1-ATPase complex, isolated from bovine heart mitochondria. (B) OCR of MCF-7 and MDA-MB-231 cells during MitoStress test (Norm MitoStress test) or modified MitoStress test (Thio MitoStress test). (C) Mitochondrial parameters obtained from normal (black bars) and modified (blue bars) MitoStress tests. ATP-linked OCR was calculated as $OCR_{before\ oligomycin\ injection}$ - $OCR_{after\ oligomycin\ injection}$. Maximal respiration was calculated as $OCR_{before\ Rot/Ant.A\ injection}$ - $OCR_{after\ Rot/Ant.A\ injection}$. Values represent mean ± SEM of three independent experiments. P value < 0.05, ***P value < 0.001.

fundamental step in the growth, invasion and metastasis of malignant tumors [22,23]. On this basis, we investigated the ability of thioalbamide to modulate the secretion of matrix metalloproteinase 9. A zymographic analysis enabled the quantification of secreted MMP-9 levels in the culture medium of MCF-7 and MDA-MB-231 tumor cell lines upon treatment with thioalbamide for 24 or 48 h, both in basal conditions and after stimulation with PMA, a pro-tumor agent that modulates the expression of metalloproteinases by activating the protein kinase C pathway (PKC) [24,25]. The results obtained (Figure 3) displayed that under basal conditions MMP-9 was not secreted by MCF-7 cells, at least at levels detectable by zymography, consistent with literature data [26]. Conversely, in the presence of PMA the

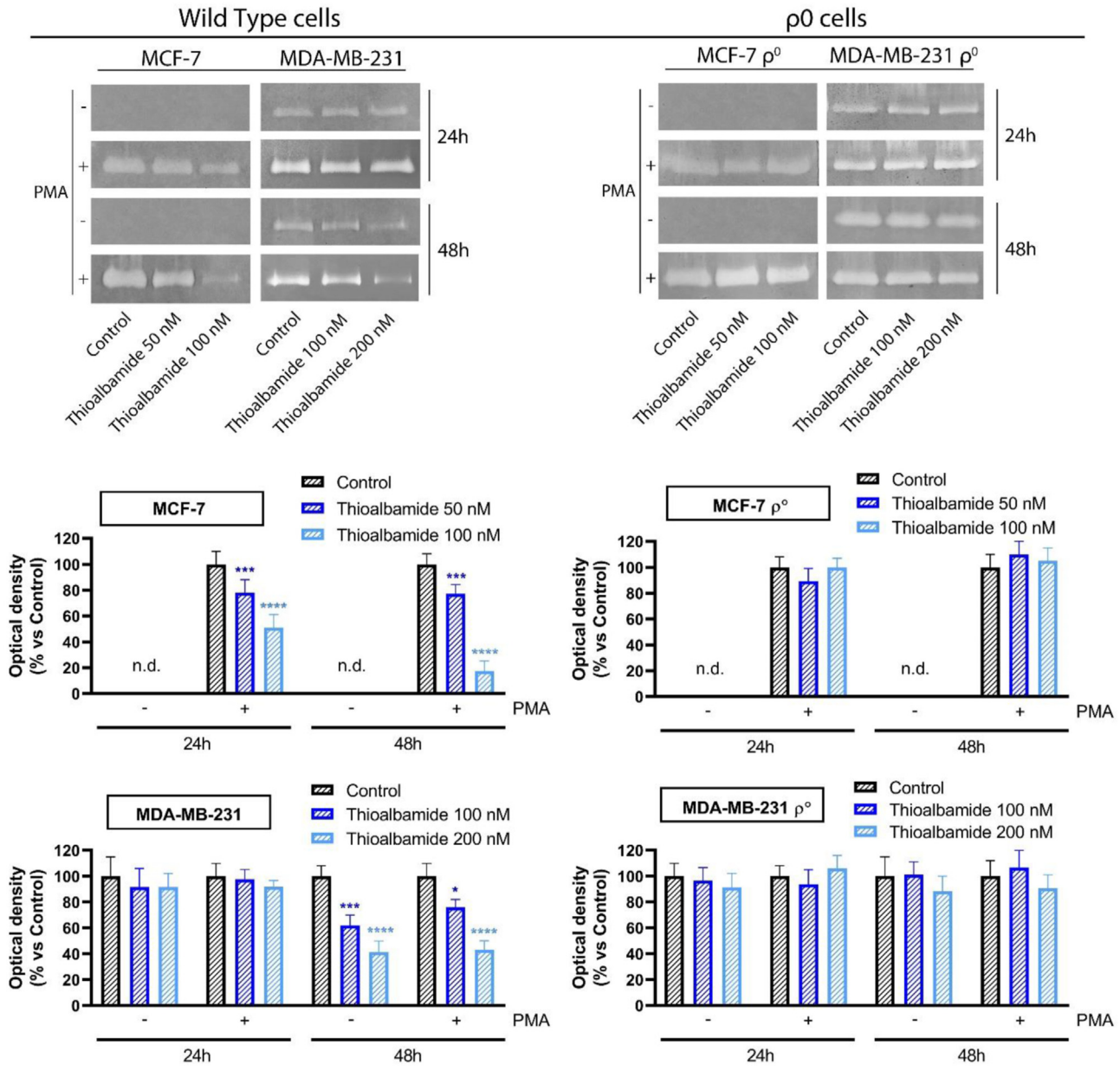

Figure 3: Thioalbamide reduces MMP-9 secretion in MCF-7 and MDA-MB-231 cells, but not in ρ^0 cell lines. MMP-9 secretion was assessed, by gelatin zymography, in conditioned medium from cells treated with DMSO (Control) or thioalbamide for 24/48 h, both in the presence or absence of PMA. Values represent mean ± SD of three independent experiments. *P value < 0.05, ***P value < 0.001, ****P value < 0.0001, n.d.: not detectable.

secreted MMP-9 level drastically increased. Thioalbamide treatment was found to reduce MMP-9 secretion in a dose-dependent manner, already after 24 h of treatment. On the other hand, MDA-MB-231 cells were able to secrete high levels of MMP-9, even in the absence of PMA stimulation, consistent with the much more aggressive nature of this cell line. Also in this case, thioalbamide was able to reduce the levels of MMP-9 secreted by tumor cells in a dose-dependent manner, although a statistically significant reduction was observed only after 48 h of treatment.

Since we identified F_0F_1-ATPase complex as a molecular target of thioalbamide, in order to further deepen the study on the modulation of MMP-9 secretion by this natural peptide, we investigated whether its effect on this marker of tumor invasiveness was due to its action at the oxidative phosphorylation level. For this reason, zymographic analysis of MMP-9 levels was carried out on the conditioned media of MCF-7 ρ^0 and MDA-MB-231 ρ^0 cells treated with thioalbamide for 24 and 48 h, in the presence or absence of PMA. The results obtained (Figure 3) showed that thioalbamide was not able to significantly reduce MMP-9 secretion in cell lines characterized by impaired OXPHOS. Hence, our results link thioalbamide effect on the secretion of matrix metalloproteinases to its action on oxidative phosphorylation system.

MMP-9 secretion by tumor cells is directly related to their invasive capacity [27,28]. Since thioalbamide is able to reduce MMP-9 secretion, we decided to confirm the effects of this microbial peptide on the invasiveness of MCF-7 and MDA-MB-231 cells, by cell invasion assay. This technique evaluates the ability of cells to digest extracellular matrix and to cross a septum with micrometric pores, thus mimicking *in vitro* the initial phases of the neoplastic dissemination

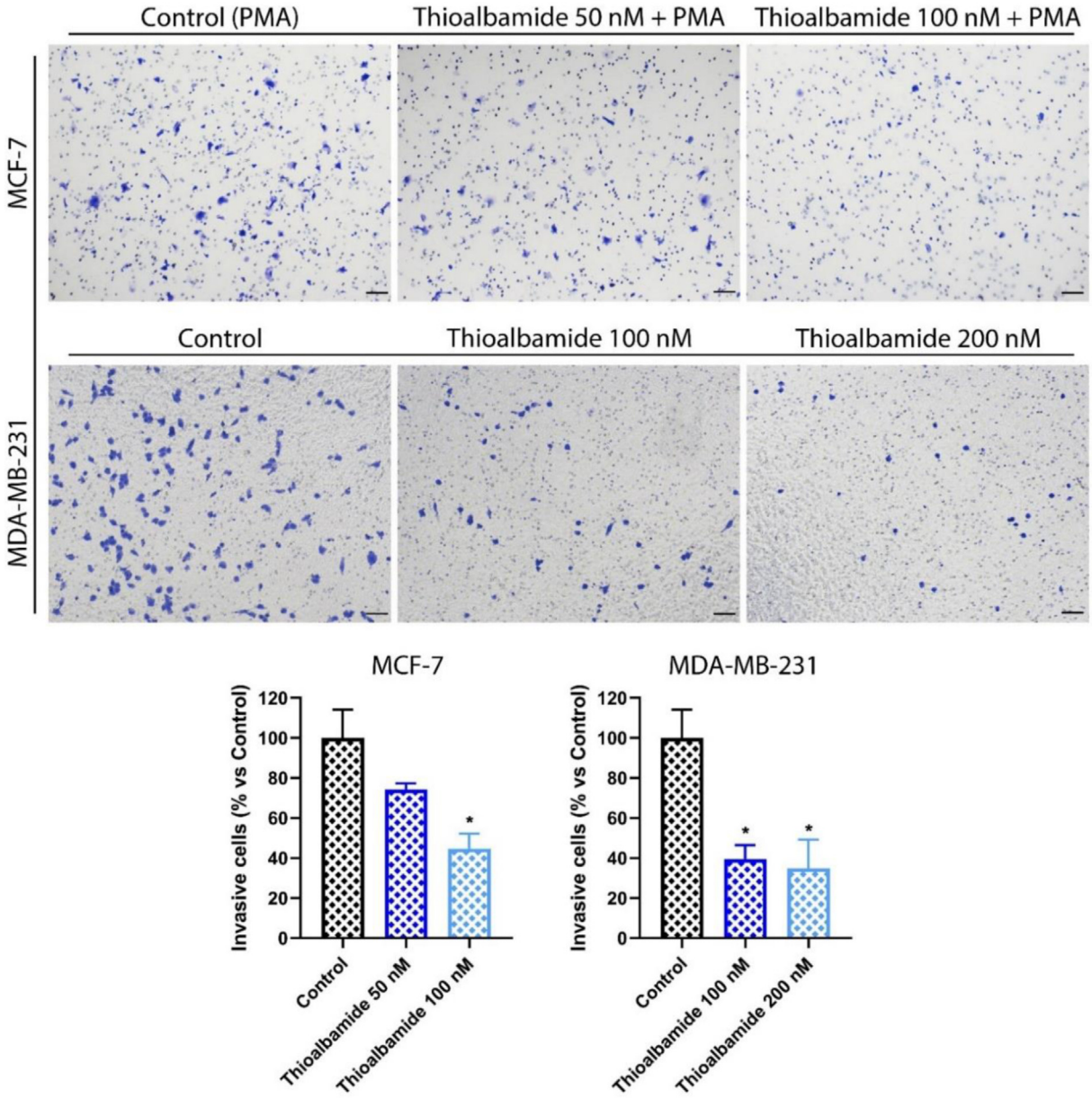

Figure 4: Thioalbamide reduces tumor invasiveness in MCF-7 and MDA-MB-231 cells. Cells were treated for 24 h with DMSO (Control) or thioalbamide as indicated, and tested for their invasive capacity. Histograms display the percentage of invasive cells vs Control. Values represent mean ± SD of three independent experiments. *P value < 0.05. *Scale bars* = 50 μm.

process. As reported in Figure 4, our results confirmed thioalbamide ability to reduce cell invasiveness and infiltration capacity in both tumor cell models used.

3.4. Thioalbamide inhibits tumor growth and stemness in breast cancer xenograft mouse models

In order to confirm the high antitumor potential of thioalbamide, we then assessed its effects *in vivo*, using tumor xenograft models. To this end, MCF-7 and MDA-MB-231 cells were ectopically inoculated in athymic nude mice, which were subsequently treated with thioalbamide (0.5 mg/kg) three times a week, via intraperitoneal administration, for three weeks. Tumor progression was studied by monitoring tumor volume throughout the treatment period. Finally, animals were euthanized and the tumor masses isolated from the surrounding tissues were weighed, sectioned and subjected to histological analysis. From the results obtained it was possible to find a statistically significant reduction in tumor volume and mass in the mice treated with thioalbamide compared to those of the control group (treated exclusively with the vehicle), thus confirming the antiproliferative effects previously found *in vitro* (Figure 5A).

Immunohistochemical analyses performed on the sections of explanted tumors highlighted the ability of thioalbamide to reduce, both in MCF-7 (Allred score mean: C = 6; T = 2) and MDA-MB-231 (Allred score mean: C = 7; T = 2) xenografts, Ki-67 antigen expression levels (Figure 5B), which is a nuclear protein whose expression significantly increases in proliferating cells [29]. In addition, this microbial peptide was able to decrease the expression of TOM20 in MCF-7 (Score mean: C = +++; T = +) and MDA-MB-231 (Score mean: C = ++; T = −)

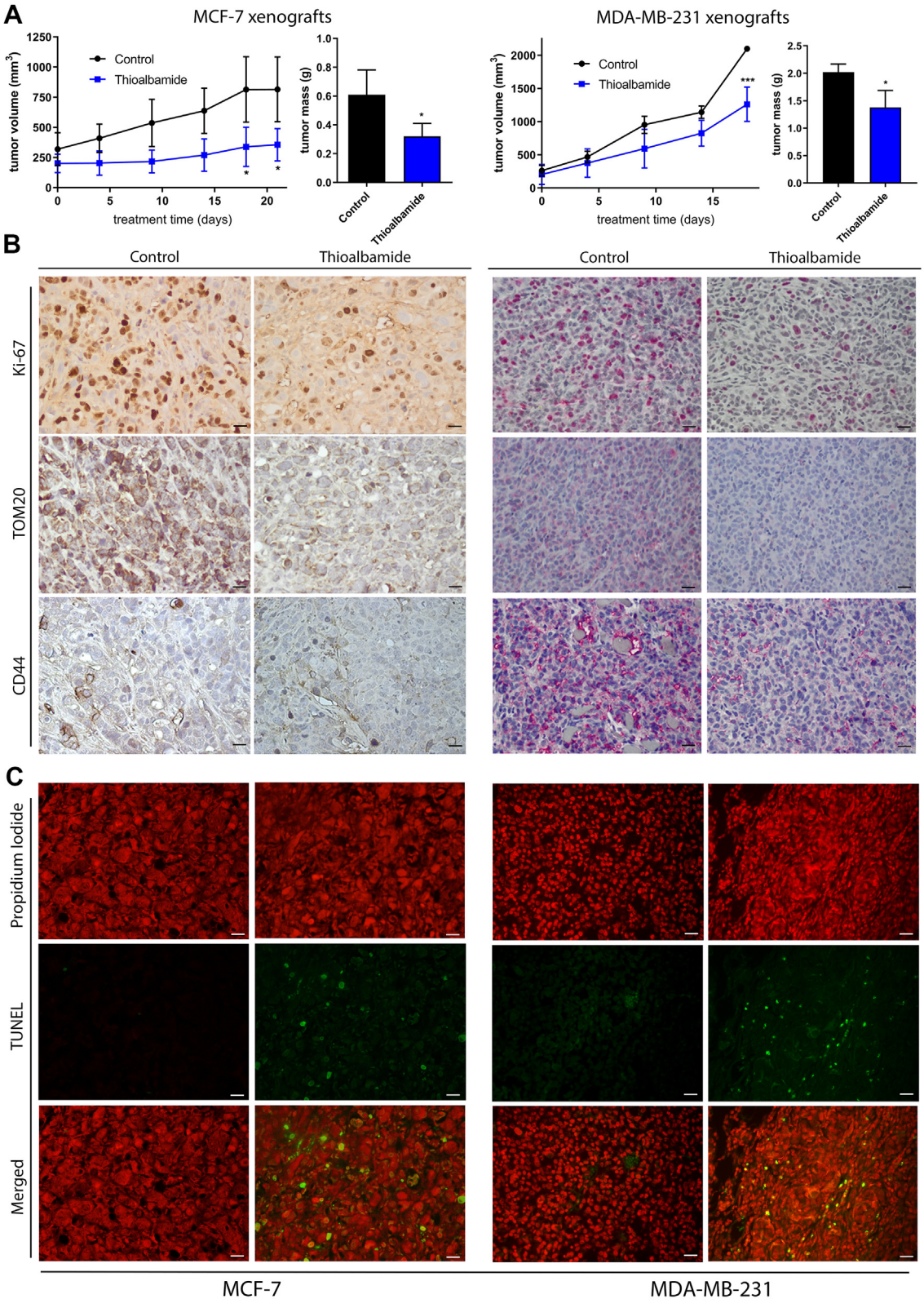

Figure 5: Thioalbamide inhibits proliferation and triggers apoptosis in breast cancer xenograft mouse models. (A) The volume of tumors was constantly monitored throughout the treatment period, whereas tumor mass was evaluated at the experimental endpoint. *P value < 0.05, ***P value < 0.001. (B) The modulation of Ki-67, TOM20 and CD44 expression was evaluated by immunohistochemistry, using DAB chromogen or Red-substrate for MCF-7 or MDA-MB-231 samples, respectively. (C) Apoptosis was assessed on MCF-7 and MDA-MB-231 tumor sections by TUNEL assay; propidium iodide was used for cell counterstaining. Both immunostaining and fluorescence from TUNEL assay were evaluated by using the Olympus BX41 microscope with CSV1.14 software, using a CAMXC-30 for image acquisition. *Scale bars* = 25 μm.

(Figure 5B), a subunit of the translocase of the outer membrane of mitochondria (TOM complex) that is part of the mitochondrial translocation machinery. This protein is considered a suitable marker of mitochondria and its expression levels can be related to the mitochondrial mass, thus confirming also *in vivo* thioalbamide effects on the mitochondrial compartment. Furthermore, the expression of the CD44 antigen, a known marker of tumor stemness [30], was also found to be strongly inhibited by thioalbamide in MCF-7 (Score mean: C = +; T = −) and particularly MDA-MB-231 (Score mean: C = +++; T = +) (Figure 5B). This effect was found to be more evident in MDA-MB-231 xenografts, since this cell line is characterized by greater intrinsic stemness and higher expression levels of this protein. These results have allowed us to confirm also *in vivo* the effects of this microbial peptide on tumor cells stemness, previously demonstrated *in vitro* [13]. Finally, the ability of thioalbamide to trigger apoptotic cell death in the tumor was demonstrated, *in vivo*, by TUNEL assay (Figure 5C), which identified cells with fragmented DNA in the sections of explanted tumors, a characteristic of cells undergoing the last stages of the apoptotic process.

3.5. Thioalbamide reduces tumor dissemination in breast cancer experimental metastasis mouse models

The ability of thioalbamide to inhibit tumor dissemination *in vivo* was investigated by using experimental metastasis mouse models, which is useful for evaluating the effects of thioalbamide *in vivo* on the ability of tumor cells, injected into the bloodstream, to generate metastases. To facilitate tumor monitoring, in mice, during neoplastic progression and metastasis dissemination, MDA-MB-231 cell line was made infrared (IR) fluorescent, so that cells were easily detectable through the use of instrumentation capable of IR fluorescent detection (Pearl Trilogy Small Animal Imaging System). The generation of a IR fluorescent cell line was achieved by performing a stable transfection of MDA-MB-231 cells with the pNLS-iRFP720 construct [31], which allows the expression of a nuclear localization protein with specific characteristics of fluorescence (excitation wavelength: 702 nm, emission wavelength: 720 nm) (Figure 6A).

Fluorescent MDA-MB-231 cells were injected into the bloodstream of the mice via the lateral caudal vein, and treatments with thioalbamide (0.5 mg/kg) were performed three times a week, via intraperitoneal administration, for five weeks. At the end of the treatment, the lung tissue was removed after perfusion with 4% paraformaldehyde, and the various organs were subjected to IR fluorescence analysis, using the Pearl Trilogy Small Animal Imaging System instrument, in order to search for the presence of metastases. As can be seen from Figure 6B, the high fluorescence of the explanted lungs from untreated mice showed that MDA-MB-231 fluorescent cells were able to generate large metastases in the lung tissue. On the other hand, the reduced fluorescence in the lungs of mice treated with thioalbamide underlines the ability of this peptide to inhibit neoplastic dissemination.

Explanted lungs were subsequently embedded in paraffin, and immuno-histochemical analysis was carried out on the obtained sections both to evaluate the morphology of the lung parenchyma and to unmask the presence of neoplastic cells by using an anti-human Ki-67 antibody. As can be seen in Figure 6C, MDA-MB-231 cells massively invaded the lung parenchyma of untreated mice, thus generating macro-metastases that completely distorted the normal morphology of the parenchyma. On the contrary, treatment with thioalbamide drastically reduced tumor invasiveness as well as the formation of macro-metastases, a result that is in full agreement with the clear difference in IR fluorescence emitted from the lungs of untreated and treated mice (Figure 6B).

4. DISCUSSION

The present study aimed to investigate the effects of thioalbamide on the bioenergetics of breast cancer cells, in order to shed light on its mechanism of action, as well as to prove its efficacy in *in vivo* experimental models, which better reflect the complexity of neoplastic pathology. Thioalbamide is a microbial peptide already known for its high antitumor potential *in vitro*, elicited at nanomolar concentrations, and for its ability to induce programmed cell death mediated by metabolic perturbations and oxidative stress. However, to date, nothing was known about its exact molecular mechanism and *in vivo* effectiveness.

This work revealed the ability of thioalbamide to exert its cytotoxic effects through a direct action on the oxidative phosphorylation process. The reduced sensitivity of breast cancer cells with impaired mitochondrial function (ρ^0 breast cancer cells), as well as the effects of thioalbamide on the activity of the enzyme complexes involved in both the electron transport chain and oxidative phosphorylation, have allowed us to presume that the effects of this microbial peptide are mainly due to its inhibitory activity towards the F_0F_1-ATPase enzyme complex. This latter is a pivotal mitochondrial multi-subunit protein complex, which drives ATP production by exploiting the proton-motive force generated through the electron transport chain.

The effects of acute thioalbamide treatment on OCR of breast cancer cells support its inhibitory activity on mitochondrial energy production pathway. In particular, the inhibitory effect observed on OCR levels, in the absence of maximal respiration alterations after FCCP injection, suggests that the activity of thioalbamide could be due to a highly selective inhibition of the F_0F_1-ATPase complex. However, further investigations are needed to establish the mechanisms through which this microbial peptide exerts its inhibitory activity. The effects of this RIPP could in fact differ from those known for oligomycin. Takase's work [15] may sustain this theory. It demonstrated the high affinity of prethioviridamide, another member of the thioamitide class of RiPP, towards the ATP5b subunit of the F_0F_1-ATPase complex, which is a catalytic subunit responsible for binding substrates, directly involved in ATP synthesis. This mechanism differs considerably from that of oligomycin, which binds the F_0 subunit of the enzyme complex, the channel that dissipates the proton gradient by favoring conformational changes and leading to ATP production through a rotational catalysis mechanism.

In this regard, a recent study has reported that MCF-7 and MDA-MB-231 cells are characterized by marked differences in OXPHOS expression levels and function, highlighting, in particular, a higher expression level of the main catalytic subunits of F_0F_1-ATPase (ATP5A, ATP5B, and ATP5C) in MCF-7 compared to MDA-MB-231 cells [32]. Since we demonstrated that thioalbamide targets the F_0F_1-ATPase complex, these metabolic differences could explain why, in our study, thioalbamide activity seems to affect more MCF-7 than MDA-MB-231 cells.

The inhibitory effects of thioalbamide, and more generally of thioamitides, on cancer cells' mitochondrial metabolism, fits well into the context in which cancer research is currently moving, since in recent years oxidative phosphorylation is emerging as a promising target in cancer treatment. Indeed, although tumors were initially considered to be purely glycolytic entities, more and more studies are re-evaluating the mitochondrial contribution in neoplastic progression [33,34]. The ability of cancer cells to shift their metabolism according to their energy needs is often responsible for the failure of antineoplastic therapies. Therefore, cancer research is increasingly focusing on targeting mitochondria and tumor metabolic plasticity, which are responsible for

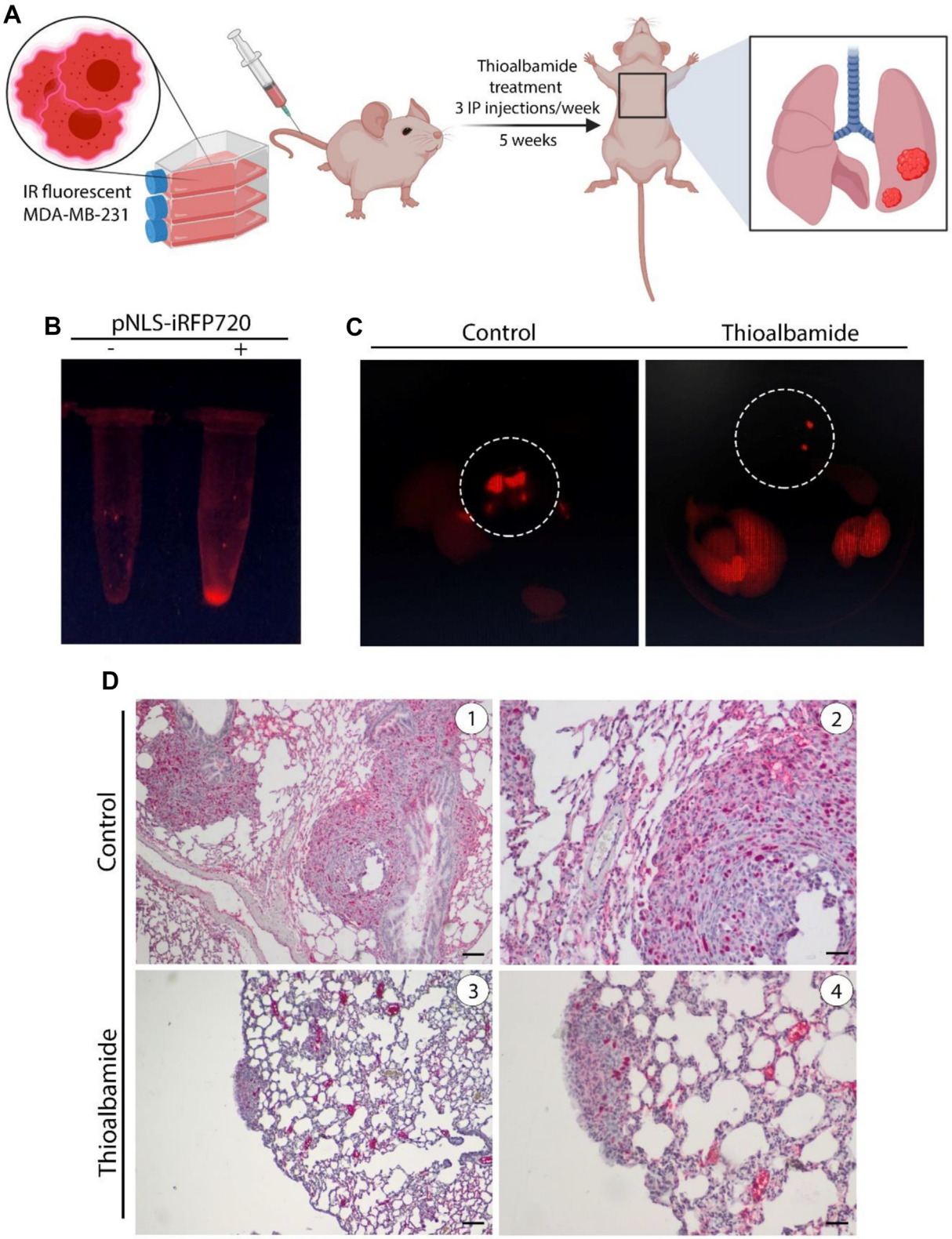

Figure 6: Thioalbamide reduces tumor dissemination in MDA-MB-231 experimental metastasis mouse models. (A) Schematic representation (Created with BioRender.com) of thioalbamide treatment of "experimental metastasis" mouse models. (B) MDA-MB-231 cells were transfected with pNLS-iRFP720 and IR fluorescence was evaluated by using the Pearl Trilogy Small Animal Imaging System. (C) IR fluorescence analysis of several organs explanted from experimental metastasis mice, by using the Pearl Trilogy Small Animal Imaging System; the white circles highlight the lungs. (D) Immunohistochemical analysis of lung sections, using the anti-human Ki-67 for metastasis detection. Immunostained slides were observed by using the Olympus BX41 microscope with CSV1.14 software, using a CAMXC-30 for image acquisition. *Scale bars:* 125 μm (d1 and d3), 50 μm (d2 and d4).

chemotherapy resistance, tumor recurrence and metastasis dissemination [35–40].

Interestingly, our findings have revealed, for the first time, the ability of thioalbamide to reduce the secretion of matrix metalloproteinase-9 by breast cancer cells. These enzymes play a key role in the digestion of the extracellular matrix, a function that makes them essential in cancer cell invasion and tumor metastasis [41,42], as well as an interesting target to be exploited in cancer treatment [43–46]. Our experimental evidence showed that the treatment of cancer cells with thioalbamide in sub-toxic conditions decreased the invasiveness of tumor cells by reducing MMP-9 secretion in the extracellular environment. This latter event can be related to the action of this microbial peptide on OXPHOS, since such an effect was not detected in treated cells deprived of mtDNA. Indeed, although ρ^0 cells, in addition to OXPHOS dysfunction, can be characterized by additional differences with parental cells, such differences are mainly consequences of the unpaired OXPHOS function.

Importantly, this study has also confirmed *in vivo* the high antitumor potential of thioalbamide. Indeed, the use of breast cancer xenograft mouse models has highlighted, even in this more complex experimental model, the ability of this peptide to trigger apoptosis, as well as to reduce tumor proliferation and cancer stemness. These results are in agreement with those detected for another thioamitide compound, thioholgamide A, which was successfully tested in xenograft zebrafish embryo models [14], and confirm the strong antitumor potential of this rare family of thioamidated microbial peptides. Furthermore, the pharmacological potential of these RiPPs is further emphasized by the new findings emerged in our investigations. Their ability to reduce *in vitro* cell migration [14] and tumor invasiveness has been successfully confirmed *in vivo*, through the use of "experimental metastasis" mouse models and IR imaging techniques. Our findings have highlighted the effect of thioalbamide in reducing the ability of cancer cells to generate metastases in the lung parenchyma, which represents the preferential metastasis site for cancer cells that reach the bloodstream. Overall, the results herein obtained have allowed us to shed more light on the molecular mechanism underlying the antitumor activity of thioalbamide. The elucidation of its effects on tumor metabolism, as well as the disclosure of its ability to reduce tumor invasiveness and neoplastic dissemination, *in vitro* and *in vivo*, can enrich the current knowledge on the biological potential of microbial thioamidated peptides, thus reducing the gap between these promising natural products and the clinical studies that could validate them as innovative anticancer agents.

FUNDING

L.F. was funded by PAC CALABRIA 2014-2020-Asse Prioritario 12, Azione B 10.5.12 CUP: H28D19000040006.

AUTHOR'S CONTRIBUTIONS

Conceptualization, L.F. and A.R.C.; Investigation, L.F., R.M., M.B. and V.R.; Data curation, L.F., R.M. and M.F.; Writing—original draft preparation, L.F. and A.R.C.; Writing—review and editing, R.C., G.L., V.D., A.W.T. and A.R.C.

ETHICS APPROVAL

All *in vivo* experiments were approved by the Animal Care Committee of University of Calabria (Italy) and the Italian Ministry of Health, under protocol no. 659/2018-PR. All animals were maintained and handled in accordance with the recommendation of the Guidelines for the Care and Use of Laboratory Animals.

CONFLICT OF INTEREST

The authors declare that they have no conflict of interests.

DATA AVAILABILITY

No data was used for the research described in the article.

REFERENCES

[1] Montalban-Lopez M, Scott TA, Ramesh S, Rahman IR, van Heel AJ, Viel JH, et al. New developments in RiPP discovery, enzymology and engineering. Nat Prod Rep 2021;38:130–239.

[2] Li Y, Liu J, Tang H, Qiu Y, Chen D, Liu W. Discovery of New Thioviridamide-Like Compounds with Antitumor Activities 2019;37:1015–20.

[3] Hayakawa Y, Sasaki K, Adachi H, Furihata K, Nagai K, Shin-ya K. Thioviridamide, a novel apoptosis inducer in transformed cells from Streptomyces olivoviridis. J Antibiot (Tokyo) 2006;59:1–5.

[4] Hayakawa Y, Sasaki K, Nagai K, Shin-ya K, Furihata K. Structure of thioviridamide, a novel apoptosis inducer from Streptomyces olivoviridis. J Antibiot (Tokyo) 2006;59:6–10.

[5] Frattaruolo L, Lacret R, Cappello AR, Truman AW. A genomics-based approach identifies a thioviridamide-like compound with selective anticancer activity. ACS Chem Biol 2017;12:2815–22.

[6] Kjaerulff L, Sikandar A, Zaburannyi N, Adam S, Herrmann J, Koehnke J, et al. Thioholgamides: thioamide-containing cytotoxic RiPP natural products. ACS Chem Biol 2017;12:2837–41.

[7] Eyles TH, Vior NM, Lacret R, Truman AW. Understanding thioamitide biosynthesis using pathway engineering and untargeted metabolomics. Chem Sci 2021;12:7138–50.

[8] Lu J, Wu Y, Li Y, Wang H. The utilization of lanthipeptide synthetases is a general strategy for the biosynthesis of 2-aminovinyl-cysteine motifs in thioamitides**. Angew Chem Int Ed Engl 2021;60:1951–8.

[9] Xiong J, Luo S, Qin CX, Cui JJ, Ma YX, Guo MX, et al. Biochemical reconstitution reveals the biosynthetic timing and substrate specificity for thioamitides. Org Lett 2022;24:1518–23.

[10] Wang C, Lu J, Zhang Y, Zheng J, Sun S, Huang S, et al. Substrate plasticity of dehydratase SpaKC from the biosynthesis of thiosparsoamide. J Pept Sci 2021: e3388.

[11] Qiu Y, Liu J, Li Y, Xue Y, Liu W. Formation of an aminovinyl-cysteine residue in thioviridamides occurs through a path independent of known lanthionine synthetase activity. Cell Chemical Biology 2021;28:675–85. e675.

[12] Sikandar A, Lopatniuk M, Luzhetskyy A, Müller R, Koehnke J. Total in vitro biosynthesis of the thioamitide thioholgamide and investigation of the pathway. J Am Chem Soc 2022;144:5136–44.

[13] Frattaruolo L, Fiorillo M, Brindisi M, Curcio R, Dolce V, Lacret R, et al. Thioalbamide, A thioamidated peptide from Amycolatopsis alba, affects tumor growth and stemness by inducing metabolic dysfunction and oxidative stress. Cells 2019:8.

[14] Dahlem C, Siow WX, Lopatniuk M, Tse WKF, Kessler SM, Kirsch SH, et al. Thioholgamide A, a new anti-proliferative anti-tumor agent, modulates macrophage polarization and metabolism. Cancers 2020:12.

[15] Takase S, Kurokawa R, Kondoh Y, Honda K, Suzuki T, Kawahara T, et al. Mechanism of action of prethioviridamide, an anticancer ribosomally synthesized and post-translationally modified peptide with a polythioamide structure. ACS Chem Biol 2019;14:1819–28.

[16] Lytle NK, Barber AG, Reya T. Stem cell fate in cancer growth, progression and therapy resistance. Nat Rev Cancer 2018;18:669–80.
[17] Brindisi M, Fiorillo M, Frattaruolo L, Sotgia F, Lisanti MP, Cappello AR. Cholesterol and mevalonate: two metabolites involved in breast cancer progression and drug resistance through the. ERRα Pathway 2020;9:1819.
[18] Casaburi I, Avena P, De Luca A, Chimento A, Sirianni R, Malivindi R, et al. Estrogen related receptor alpha (ERRalpha) a promising target for the therapy of adrenocortical carcinoma. ACC), Oncotarget 2015;6:25135–48.
[19] Rago V, Romeo F, Giordano F, Ferraro A, Andò S, Carpino A. Identification of ERbeta1 and ERbeta2 in human seminoma, in embryonal carcinoma and in their adjacent intratubular germ cell neoplasia. Reprod Biol Endocrinol: RBE (Rev Bras Entomol) 2009;7:56.
[20] Panza S, Giordano F, De Rose D, Panno ML, De Amicis F, Santoro M, et al. FSH-R human early male genital tract, testicular tumors and sperm: its involvement in testicular disorders. Basel, Switzerland): Life; 2020. p. 10.
[21] Schubert S, Heller S, Loffler B, Schafer I, Seibel M, Villani G, et al. Generation of rho zero cells: visualization and quantification of the mtDNA depletion process. Int J Mol Sci 2015;16:9850–65.
[22] de Almeida LGN, Thode H, Eslambolchi Y, Chopra S, Young D, Gill S, et al. Matrix metalloproteinases: from molecular mechanisms to physiology, pathophysiology, and pharmacology. Pharmacol Rev 2022;74:712–68.
[23] Gonzalez-Avila G, Sommer B, Mendoza-Posada DA, Ramos C, Garcia-Hernandez AA, Falfan-Valencia R. Matrix metalloproteinases participation in the metastatic process and their diagnostic and therapeutic applications in cancer. Crit Rev Oncol Hematol 2019;137:57–83.
[24] Park MJ, Park IC, Lee HC, Woo SH, Lee JY, Hong YJ, et al. Protein kinase C-alpha activation by phorbol ester induces secretion of gelatinase B/MMP-9 through ERK 1/2 pathway in capillary endothelial cells. Int J Oncol 2003;22:137–43.
[25] Shin YH, Yoon S-H, Choe E-Y, Cho S-H, Woo C-H, Rho J-Y, et al. PMA-induced up-regulation of MMP-9 is regulated by a PKCα-NF-κB cascade in human lung epithelial cells. Exp Mol Med 2007;39:97–105.
[26] Roomi MW, Monterrey JC, Kalinovsky T, Rath M, Niedzwiecki A. Patterns of MMP-2 and MMP-9 expression in human cancer cell lines. Oncol Rep 2009;21:1323–33.
[27] Tester AM, Ruangpanit N, Anderson RL, Thompson EW. MMP-9 secretion and MMP-2 activation distinguish invasive and metastatic sublines of a mouse mammary carcinoma system showing epithelial-mesenchymal transition traits. Clin Exp Metastasis 2000;18:553–60.
[28] Köhrmann A, Kammerer U, Kapp M, Dietl J, Anacker J. Expression of matrix metalloproteinases (MMPs) in primary human breast cancer and breast cancer cell lines: new findings and review of the literature. BMC Cancer 2009;9:188.
[29] Sun X, Kaufman PD. Ki-67: more than a proliferation marker. Chromosoma 2018;127:175–86.
[30] Wang L, Zuo X, Xie K, Wei D. The role of CD44 and cancer stem cells. Methods Mol Biol 2018;1692:31–42.
[31] Shcherbakova DM, Verkhusha VV. Near-infrared fluorescent proteins for multicolor in vivo imaging. Nat Methods 2013;10:751–4.
[32] Lunetti P, Di Giacomo M, Vergara D, De Domenico S, Maffia M, Zara V, et al. Metabolic reprogramming in breast cancer results in distinct mitochondrial bioenergetics between luminal and basal subtypes. FEBS J 2019;286:688–709.
[33] Porporato PE, Filigheddu N, Pedro JMB, Kroemer G, Galluzzi L. Mitochondrial metabolism and cancer. Cell Res 2018;28:265–80.
[34] Grasso D, Zampieri LX, Capeloa T, Van de Velde JA, Sonveaux P. Mitochondria in cancer. Cell Stress 2020;4:114–46.
[35] Frattaruolo L, Brindisi M, Curcio R, Marra F, Dolce V, Cappello AR. Targeting the mitochondrial metabolic network: a promising strategy in cancer treatment. Int J Mol Sci 2020;21.
[36] Guo X, Yang N, Ji W, Zhang H, Dong X, Zhou Z, et al. Mito-bomb: targeting mitochondria for cancer therapy. Adv Mater 2021;33:e2007778.
[37] Armentano B, Curcio R, Brindisi M, Mancuso R, Rago V, Ziccarelli I, et al. 5-(Carbamoylmethylene)-oxazolidin-2-ones as a promising class of heterocycles inducing apoptosis triggered by increased ROS levels and mitochondrial dysfunction in breast and cervical cancer. Biomedicines 2020;8.
[38] Pustylnikov S, Costabile F, Beghi S, Facciabene A. Targeting mitochondria in cancer: current concepts and immunotherapy approaches. Transl Res 2018;202:35–51.
[39] Skoda J, Borankova K, Jansson PJ, Huang ML, Veselska R, Richardson DR. Pharmacological targeting of mitochondria in cancer stem cells: an ancient organelle at the crossroad of novel anti-cancer therapies. Pharmacol Res 2019;139:298–313.
[40] Vasan K, Werner M, Chandel NS. Mitochondrial metabolism as a target for cancer therapy. Cell Metabol 2020;32:341–52.
[41] Mehner C, Hockla A, Miller E, Ran S, Radisky DC, Radisky ES. Tumor cell-produced matrix metalloproteinase 9 (MMP-9) drives malignant progression and metastasis of basal-like triple negative breast cancer. Oncotarget 2014;5:2736–49.
[42] Joseph C, Alsaleem M, Orah N, Narasimha PL, Miligy IM, Kurozumi S, et al. Elevated MMP9 expression in breast cancer is a predictor of shorter patient survival. Breast Cancer Res Treat 2020;182:267–82.
[43] Owyong M, Chou J, van den Bijgaart RJ, Kong N, Efe G, Maynard C, et al. MMP9 modulates the metastatic cascade and immune landscape for breast cancer anti-metastatic therapy, 2. Life Sci Alliance; 2019.
[44] Mondal S, Adhikari N, Banerjee S, Amin SA, Jha T. Matrix metalloproteinase-9 (MMP-9) and its inhibitors in cancer: a minireview. Eur J Med Chem 2020;194:112260.
[45] Allen JL, Hames RA, Mastroianni NM, Greenstein AE, Weed SA. Evaluation of the matrix metalloproteinase 9 (MMP9) inhibitor Andecaliximab as an Anti-invasive therapeutic in Head and neck squamous cell carcinoma. Oral Oncol 2022;132:106008.
[46] Zhu Y, Huang R-Z, Wang C-G, Ouyang X-L, Jing X-T, Liang D, et al. New inhibitors of matrix metalloproteinases 9 (MMP-9): lignans from Selaginella moellendorffii. Fitoterapia 2018;130:281–9.

